

Homogenized Upper Bound FE limit analysis model for FRP-reinforced masonry vaults

Gabriele Milani¹, Enrico Milani², Antonio Tralli²

¹*Dipartimento di Ingegneria Strutturale (DIS), Politecnico di Milano, Milan, Italy*
E-mail: gabriele.milani@polimi.it

²*Dipartimento di Ingegneria, Università di Ferrara, Ferrara, Italy*
E-mail: enrico.milani@unife.it, atralli@ing.unife.it

Keywords: Masonry, FRP-reinforcement, limit analysis, upper bound, homogenization.

SUMMARY. A homogenized full 3D limit analysis model for the evaluation of collapse loads of FRP-reinforced masonry vaults is presented. A two steps approach is adopted in the paper; in step I, a simplified kinematic procedure is proposed at a cell level to obtain macroscopic masonry behavior in the case of unreinforced masonry curved structures, whereas in step II strips are applied at a structural level on the already homogeneous material.

Six-noded rigid infinitely resistant wedges are used to model masonry. Three-noded rigid infinitely resistant triangles are used to model FRP strips. Plastic dissipation is allowed only at the interfaces between adjoining elements. Masonry ultimate strength is evaluated through an admissible rigid-plastic homogenization model, where joints are reduced to interfaces with frictional behavior and bricks are assumed obeying a Mohr-Coulomb failure criterion and are modeled by means of six noded infinitely resistant wedge shaped limit analysis elements with possible dissipation at the interfaces. The curved representative element of volume (REV) is constituted by a central brick interconnected with its six neighbors. A recently presented compatible identification procedure is finally adopted on the REV, a priori assuming a sub-class of macroscopic deformation modes on the REV and equating power dissipated in the heterogeneous model to power dissipated in a continuous homogeneous plate. A fast and reliable FE estimation of masonry homogenized failure surfaces when loaded in- and out-of-plane is thus obtained.

At a structural level, a possible dissipation at the interfaces between FRP triangles and masonry wedges is considered in order to take into account, in an approximate but effective way, the possible delamination of the strips from the support. Italian code formulas are used to evaluate peak interface tangential strength. A numerical example is analyzed in order to evaluate the capabilities of the model proposed, relying on a hemispherical masonry structure reinforced with hooping FRP strips. For the example presented, both the unreinforced and FRP reinforced case are discussed in order to have a deep insight into the efficiency of the strengthening intervention proposed. Additional non-linear FE analyses are performed, modeling masonry through an equivalent macroscopic material with orthotropic behavior at failure and possible softening, in order to assess limit analysis results. Comparisons with experimental evidences, where available, are finally reported. Reliable predictions of collapse loads and failure mechanisms are obtained with the model proposed, meaning that the approach proposed may be used by practitioners for a fast and reliable evaluation of the effectiveness of a strengthening intervention.

1 INTRODUCTION

The recent earthquakes occurred in Umbria and Marche (Italy 1997-1998), Molise (Italy 2002) and Abruzzo (Italy 2009) indicated that the historical Italian buildings, essentially constituted by

masonry structures, are scarcely resistant to horizontal loads and highly vulnerable to seismic actions [1]. Such inadequate behavior of brickwork under earthquakes is a common issue of masonry buildings in many countries worldwide. Inadequate resistance under seismic actions may be observed also for curved masonry structures, as for instance vaults, domes and arches, which typically are designed to withstand vertical loads under membranal regimes only. Conventional retrofitting techniques, such as external reinforcement with steel plates, surface concrete coating and welded mesh, have proven to be impractical, time expensive and add considerable mass to the structure (which may increase earthquake-induced inertia forces). In this context, the utilization of FRP strips as reinforcement instead of conventional methods seems the most suitable solution for their limited invasiveness, durability and good performance at failure.

Nevertheless, it is worth noting that, despite the great importance and the increasing diffusion of such innovative strengthening technique, few numerical models devoted to the prediction of the ultimate load bearing capacity of out-of-plane loaded FRP-reinforced masonry are nowadays at disposal. Furthermore, when dealing with curved masonry structures, the complex interaction between membrane and flexural actions is very complex and brings additional complexity to the structural analyses.

As well known, limit analysis (a valuable alternative to expensive non-linear FE simulations) has been widely used for the analysis at failure of masonry structures (e.g. Heyman [2], Sinha [3], Orduna and Lourenço [4], etc.), because it requires only a reduced number of material parameters, providing limit multipliers of loads, failure mechanisms and, at least on critical sections, the stress distribution at collapse.

Reliable results have been obtained also in the specific case of curved structures (see for instance Heyman [2], Milani et al. [5]). Very recently, limit state approaches have been attempted for masonry arches also in presence of FRP reinforcement strips, see e.g. Caporale et al. [6].

As a matter of fact, non linear complex damaging models should be used for the analysis FRP reinforced masonry. The FRP delamination from the support is, indeed, typically brittle, as well as the tensile cracking of mortar joints. These aspects preclude, in principle, the utilization of limit analysis, which is based on the assumption of perfect plasticity for the constituent materials.

Despite the aforementioned limitations connected to the hypotheses at the base of the approach proposed, following also what suggested in the Italian Code CNR-DT200 [7], limit analysis may be useful for design purposes, to provide a fast and reliable estimation of collapse loads at a structural level and the change in the failure mechanism when FRP strips are inserted to preclude the formation of premature mechanisms.

The most important effect of a generic strengthening intervention executed with FRP strips is, indeed, to preclude the formation of the failure mechanism which causes the collapse of the unreinforced structure, with the subsequent formation of a new collapse mechanism different from the un-strengthened case, with higher internal dissipation. Obviously, "hand" calculations may not be performed easily for complex structures, especially in presence of curved shells with unsymmetrical loads. Therefore, the adoption of an upper bound approach combined with FEM seems particularly suited for the prediction of FRP-masonry behavior prone to collapse. A homogenized full 3D limit analysis model for the evaluation of collapse loads of FRP-reinforced masonry vaults has been presented by the Authors in [8], where six-noded rigid infinitely resistant wedges to model masonry and three-noded rigid infinitely resistant triangles to model FRP strips have been used.

In this paper, some of the simulations performed in [8] are concisely reviewed and a numerical example is discussed, consisting of a masonry dome with annular reinforcement. For the example presented, both the unreinforced and FRP reinforced case are discussed. Additional non-linear FE

analyses are performed (DIANA 9.2) modeling masonry through an equivalent macroscopic material with orthotropic behavior at failure and possible softening, in order to assess limit analysis results. Comparisons with experimental evidences, where available, are finally reported.

Reliable predictions of collapse loads and failure mechanisms are obtained with the model proposed for the analyzed structure [9], meaning that the approach proposed may be used by practitioners for a fast and reliable evaluation of the effectiveness of a strengthening intervention.

2 HOMOGENIZATION OF RIGID-PLASTIC CURVED MASONRY STRUCTURES

The kinematic definition of S^{hom} , used in this paper, is obtained following the general procedure suggested by Suquet [10], i.e. assuming in the elementary cell a velocity field \mathbf{v} equal to $\dot{\tilde{\mathbf{E}}}\mathbf{y} + \dot{\tilde{\boldsymbol{\chi}}}\mathbf{y} + \dot{\tilde{\boldsymbol{\Gamma}}}\mathbf{y} + \mathbf{v}^{\text{per}}$, where $\dot{\tilde{\mathbf{E}}}$ is a macroscopic strain rate field, $\dot{\tilde{\boldsymbol{\chi}}}$ contains the macroscopic curvature rate field, $\dot{\tilde{\boldsymbol{\Gamma}}}$ contains the macroscopic out-of-plane sliding rate, and \mathbf{v}^{per} is a periodic velocity field. Under these hypotheses, the so called support function π^{hom} can be evaluated as follows:

$$\pi^{\text{hom}}(\dot{\tilde{\mathbf{E}}}, \dot{\tilde{\boldsymbol{\chi}}}, \dot{\tilde{\boldsymbol{\Gamma}}}) = \inf_{\mathbf{v}} \left\{ P(\mathbf{v}) \mid \mathbf{v} = \dot{\tilde{\mathbf{E}}}\mathbf{y} + \dot{\tilde{\boldsymbol{\chi}}}\mathbf{y} + \dot{\tilde{\boldsymbol{\Gamma}}}\mathbf{y} + \mathbf{v}^{\text{per}} \right\} \quad (1)$$

Where $P(\mathbf{v})$ is the power dissipated in the elementary cell for a given \mathbf{v} .

It has been shown (see for details Suquet [10] and [5]) that a kinematic definition of S^{hom} can be obtained as follows:

$$S^{\text{hom}} \equiv (\mathbf{N} \ \mathbf{M} \ \mathbf{T}) \mid \left\{ \begin{array}{l} \mathbf{N} : \dot{\tilde{\mathbf{E}}} + \mathbf{M} : \dot{\tilde{\boldsymbol{\chi}}} + \mathbf{T}^T \dot{\tilde{\boldsymbol{\Gamma}}} = 1 \leq \pi^{\text{hom}}(\dot{\tilde{\mathbf{E}}}, \dot{\tilde{\boldsymbol{\chi}}}, \dot{\tilde{\boldsymbol{\Gamma}}}) \quad \forall \dot{\tilde{\mathbf{E}}}, \dot{\tilde{\boldsymbol{\chi}}}, \dot{\tilde{\boldsymbol{\Gamma}}} \\ \pi^{\text{hom}}(\dot{\tilde{\mathbf{E}}}, \dot{\tilde{\boldsymbol{\chi}}}, \dot{\tilde{\boldsymbol{\Gamma}}}) = \inf_{\mathbf{v}} \left\{ P(\mathbf{v}) \mid \mathbf{v} = \dot{\tilde{\mathbf{E}}}\mathbf{y} + \dot{\tilde{\boldsymbol{\chi}}}\mathbf{y} + \dot{\tilde{\boldsymbol{\Gamma}}}\mathbf{y} + \mathbf{v}^{\text{per}} \right\} \\ P(\mathbf{v}) = \int_Y \pi(\dot{\mathbf{d}}) dY + \int_S \pi([\boldsymbol{\sigma}]; \mathbf{n}) dS \end{array} \right. \quad (2)$$

where:

- S is any discontinuity surface of \mathbf{v} in the unit cell Y , \mathbf{n} is the normal to the discontinuity surface S ;
- $\pi([\boldsymbol{\sigma}]; \mathbf{n}) = 1/2([\boldsymbol{\sigma}] \otimes \mathbf{n} + \mathbf{n} \otimes [\boldsymbol{\sigma}])$;
- $\pi(\dot{\mathbf{d}}) = \max_{\boldsymbol{\sigma}} \{ \boldsymbol{\sigma} : \dot{\mathbf{d}}; \boldsymbol{\sigma} \in S(\mathbf{y}) \}$;
- \mathbf{N} , \mathbf{M} and \mathbf{T} are the ultimate homogenized membrane, bending and out-of-plane shear actions respectively.

In the model, masonry ultimate strength is evaluated through a FE upper bound limit analysis homogenization approach, where joints are reduced to interfaces with frictional behavior and limited tensile and compressive strength and bricks are assumed obeying a Mohr-Coulomb failure criterion and are modeled by means of six noded infinitely resistant wedge shaped limit analysis elements with possible dissipation at the interfaces. The curved representative element of volume (REV) is constituted by a central brick interconnected with its six neighbors, see Figure 1. A recently presented compatible identification procedure (the reader is referred to [8] for a detailed discussion of the model) is finally adopted on the REV, a priori assuming a sub-class of macroscopic deformation modes on the REV and equating power dissipated in the heterogeneous model to power dissipated in a continuous homogeneous plate. A fast and reliable FE estimation

of masonry homogenized failure surfaces when loaded in- and out-of-plane is thus obtained.

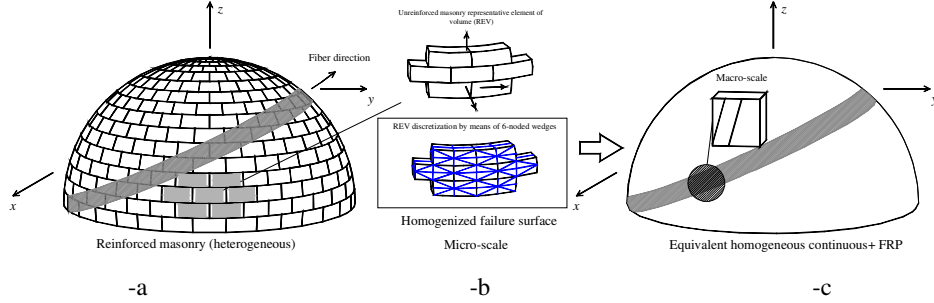


Figure 1: Two steps approach adopted. –a: reinforced heterogeneous structure. –b: micro-scale, unreinforced kinematic approach. –c: macro-scale, FRP-reinforced masonry material.

3 THE STRUCTURAL LEVEL F. E. MODEL: BASIC ASSUMPTIONS

The simplest FE discretization of a curved masonry structure reinforced with FRP strips is represented by a piecewise linear approximation of the middle surface by means of rigid flat six-noded wedge elements. The utilization of wedges (i.e. 3D elements) instead of plate and shell triangles for masonry is useful to reproduce the flexural behavior of the structures when a surface reinforcement with FRP strips is introduced. This approach has, indeed, the further advantage of (1) automatically distinguishing between intrados and extrados reinforcement and (2) requiring only in-plane and out-of-plane shear homogenized masonry failure surfaces, since flexural behavior is derived at a structural level by integration along the thickness.

In this framework, the less expensive limit analysis approach which may be proposed is a model with rigid infinitely resistant wedges. Thus, following a general approach widely diffused in the technical literature for masonry plates out-of-plane loaded (see e.g. Sinha [3]), in the model, plastic dissipation is allowed only at the interfaces between adjoining elements.

3.1 6-noded wedge masonry element

A 6-noded wedge element E utilized for bricks discretization at a cell level is used at a structural level to model homogenized masonry. Kinematic variables for each wedge element are represented by three centroid velocities (u_x^E, u_y^E, u_z^E) and three rotations around centroid G ($\Phi_x^E, \Phi_y^E, \Phi_z^E$), Figure 2. Γ_{12}^e edge surface of an element E , connecting P_1, P_2, P_4 and P_5 nodes is rectangular and jump of velocities on it is linear. In particular, velocity field of a generic point P with global coordinates (x_P, y_P, z_P) , on Γ_{12}^E is expressed in the global frame of reference as:

$$\mathbf{U}(P) = \begin{bmatrix} u_x \\ u_y \\ u_z \end{bmatrix} = \begin{bmatrix} u_x^G \\ u_y^G \\ u_z^G \end{bmatrix} + \begin{bmatrix} 0 & -\Phi_y^G & \Phi_z^G \\ \Phi_y^G & 0 & -\Phi_x^G \\ -\Phi_z^G & \Phi_x^G & 0 \end{bmatrix} \begin{bmatrix} x_P - x_G \\ y_P - y_G \\ z_P - z_G \end{bmatrix} = \mathbf{U}_E^G + \mathbf{R}_E(P - G) \quad (3)$$

Where $\mathbf{U}(P)$ is the point P velocity, \mathbf{U}_E^G is the element E centroid velocity and \mathbf{R}_E is

element E rotation matrix.

From equation (3), jump of displacements $[\mathbf{U}(P)]$ at a point P on the interfaces I between two contiguous elements N and M can be evaluated as difference between velocities of P regarded belonging respectively to N and M :

$$[\mathbf{U}(P)] = \mathbf{U}_M^G - \mathbf{U}_N^G + \mathbf{R}_M(P - G_M) - \mathbf{R}_N(P - G_N) \quad (4)$$

We introduce for each interface I between contiguous elements the vector field \mathbf{t}^I , defined as $\mathbf{t}^{I^T} = [\tau_1^I \quad \tau_2^I \quad \sigma_s^I]$ and representing the stress acting along local axis $\mathbf{r}_1^I(\tau_1^I)$, $\mathbf{r}_2^I(\tau_2^I)$ and $\mathbf{s}^I(\sigma_s^I)$, as indicated in Figure 2.

Power dissipated at the interface can be evaluated analytically as:

$$P^I = \int_0^{\Omega_{12}} (\sigma_{r1}^I \Delta r_1 + \sigma_{r2}^I \Delta r_2 + \sigma_s^I \Delta s) d\Omega \quad (5)$$

Where Δr_1 , Δr_2 and Δs are velocities jumps (two tangential and mutually orthogonal and one perpendicular to the interface, see Figure 2) in the local coordinate system $\mathbf{r}_1^I - \mathbf{r}_2^I - \mathbf{s}^I$. Velocities jumps in the local system may be easily evaluated from (4) once that the rotation matrix \mathbf{R}^I for $\mathbf{r}_1^I - \mathbf{r}_2^I - \mathbf{s}^I$ is evaluated:

$$\Delta \mathbf{U}(P) = \mathbf{R}^I [\mathbf{U}(P)] \quad (6)$$

Where $\Delta \mathbf{U}(P)$ is the jump of velocities vector in the local system.

For each interface I of area Ω_{12} connecting nodes 1-2-3-4 (Figure 2), we suppose to have at disposal a homogenized (linearized) strength domain in the local coordinate system $\mathbf{r}_1^I - \mathbf{r}_2^I - \mathbf{s}^I$ and constituted by m^I planes. Such a linearization for each interface (and, in principle, for each point of the interface) can be obtained from S^{hom} applying the procedure recommended by Krabbenhoft et al. [11], and the reader is referred there for further details.

In particular, we assume that a generic linearization plane q^I has equation $A_{r1}^{q^I} \tau_1^I + A_s^{q^I} \sigma_s^I + A_{r2}^{q^I} \tau_2^I = C_i^{q^I}$ $1 \leq q^I \leq m^I$. Introducing plastic multipliers fields at the interface (one for each linearization plane), from equations (5), power dissipated at the interface can be rewritten as:

$$P^I = \int_0^{\Omega_{12}} \sum_{q^I} \dot{\lambda}_i^{q^I}(r_1, r_2) (A_{r1}^{q^I} \tau_1^I + A_s^{q^I} \sigma_s^I + A_{r2}^{q^I} \tau_2^I) ds \quad (7)$$

Obviously, field $\dot{\lambda}_i^{q^I}(r_1, r_2)$ assumes the same analytical expression found for the velocity field, i.e. is linear in $r_1 - r_2$, see equation (6). Therefore, $\dot{\lambda}_i^{q^I}(r_1, r_2)$ field is fully determined introducing only three plastic multipliers for each internal interface and for each linearization plane, corresponding e.g. to nodes 1, 4, 2.

External power dissipated can be written as $P^{\text{ex}} = (\mathbf{P}_0^T + \lambda \mathbf{P}_1^T) \mathbf{w}$, where \mathbf{P}_0 is the vector of permanent loads, λ is the load multiplier for the structure examined, \mathbf{P}_1^T is the vector of variable loads and \mathbf{w} is the vector of assembled centroid elements velocities. As the amplitude of the failure mechanism is arbitrary, a further normalization condition $\mathbf{P}_1^T \mathbf{w} = 1$ is usually introduced.

Hence, the external power becomes linear in \mathbf{W} and λ .

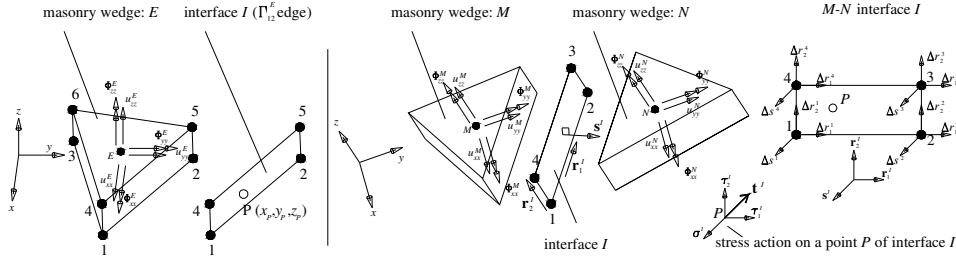


Figure 2: Masonry six-noded wedge element (left) and four-noded interface (right) between contiguous masonry elements (global and local frame of reference).

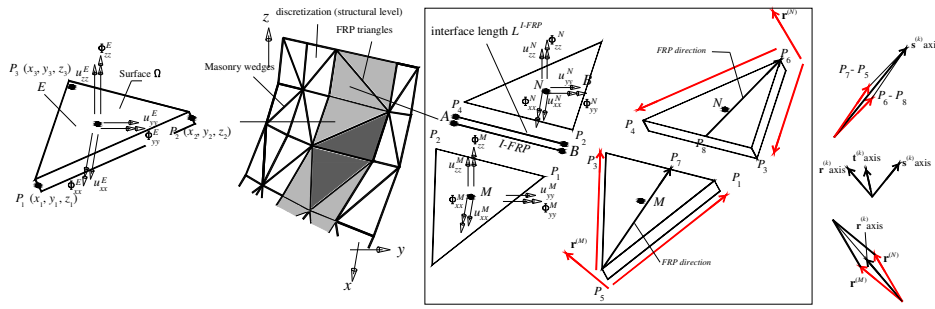


Figure 3: FRP triangular element (left) and A-B interface between two contiguous M-N triangular FRP elements (right) with corresponding local frame of reference (a possible jump of velocities along FRP direction may occur at A-B).

3.2.3 3-noded flat FRP elements (triangles)

Three-noded triangular shell elements are utilized to model FRP strips, with nodes coordinates $P_i = (x_i, y_i, z_i)$, $i = 1, \dots, 3$ and node numbers disposed in counter clockwise. Let symbol Ω indicates the surface of a FRP element E , Figure 3.

Analogously to wedge masonry elements, FRP triangles are supposed infinitely resistant and rigid. Therefore, plastic dissipation is allowed only at the interfaces between contiguous elements due to stresses acting on the fibers direction. Continuity of the velocity field is imposed at each interface between contiguous FRP triangular elements only along directions $\mathbf{r}^{(k)}$ and $\mathbf{t}^{(k)}$ (see Figure 3) whereas a possible jump of velocities is supposed to occur along direction $\mathbf{s}^{(k)}$.

With reference to Figure 3, let two contiguous FRP elements M and N be considered. Their centroid velocities and rotation rates are $\mathbf{u}^M = [u_{xx}^M \ u_{yy}^M \ u_{zz}^M]^T$, $\mathbf{u}^N = [u_{xx}^N \ u_{yy}^N \ u_{zz}^N]^T$, $\Phi^M = [\Phi_{xx}^M \ \Phi_{yy}^M \ \Phi_{zz}^M]^T$ and $\Phi^N = [\Phi_{xx}^N \ \Phi_{yy}^N \ \Phi_{zz}^N]^T$. Jump of velocities on the common M and N interface ($I - FRP$) is linear: therefore, it is necessary to evaluate jump of velocities only on the interface extremes A and B as difference between velocities of nodes 1-3 and 2-4

respectively.

As a rule, low compressive stresses induce buckling of the strips, due to the FRP negligible thickness. In order to take into account this effect (at least in an approximate way), different limit stresses are assumed in tension and compression, namely f_{FRP}^+ (assumed equal to f_{jdd} or $f_{jdd,rid}$ in agreement with CNR-DT200 [7], see the following section for details) for tensile failure and $f_{FRP}^- \approx 0$ for compression buckling respectively.

To be kinematically admissible, velocity jump at the interfaces must obey an associated flow rule:

$$[\mathbf{u}_i] = [\Delta u_s^i \quad \Delta u_r^i \quad \Delta u_t^i]^T = [\dot{\lambda}_i^{I-FRP+} - \dot{\lambda}_i^{I-FRP-} \quad 0 \quad 0]^T \quad (8)$$

Where $i = A$ or B and $\dot{\lambda}_i^{I-FRP+}$ and $\dot{\lambda}_i^{I-FRP-}$ are plastic multiplier rates of point i (interface $I - FRP$) corresponding to f_{FRP}^+ and f_{FRP}^- respectively.

On the other hand, within each interface $I - FRP$ of length L^{I-FRP} (thickness s), the power dissipated may be easily evaluated as:

$$\begin{aligned} \pi^F &= \frac{L^{I-FRP}}{2} (\Delta u_s^A \sigma_A + \Delta u_s^B \sigma_B) = \\ &= \frac{L^{I-FRP}}{2} (f_{FRP}^+ (\dot{\lambda}_A^{I-FRP+} + \dot{\lambda}_B^{I-FRP+}) + f_{FRP}^- (\dot{\lambda}_A^{I-FRP-} + \dot{\lambda}_B^{I-FRP-})) \end{aligned} \quad (9)$$

Where σ_A and σ_B represent stress action along $\mathbf{s}^{(k)}$ on nodes A and B .

3.3 FRP/masonry interfaces (delamination)

In the Italian norm, a simplified approach is proposed to evaluate the delamination phenomenon, suitably limiting force action on the FRP strip. In particular, the f_{jdd} design tensile strength of FRP elements is:

$$f_{jdd} = \frac{1}{\gamma_{fd} \sqrt{\gamma_M}} \sqrt{\frac{2 \cdot E_{FRP} \cdot \Gamma_{Fk}}{t_{FRP}}} \quad (10)$$

if the so called bond length l_b is greater than the optimal bond length l_e or:

$$f_{jdd,rid} = f_{jdd} \frac{l_b}{l_e} \left(2 - \frac{l_b}{l_e} \right) \quad (11)$$

if $l_b \leq l_e$.

In equations (10) and (11), $f_{jdd,rid}$ is the reduced value of the design bond strength, f_{jdd} the design bond strength, E_{FRP} the FRP Young modulus, t_{FRP} the FRP thickness, f_d a safety factor (in what follows it is assumed equal to 1.20), γ_M is a partial safety factor for masonry assumed in the following equal to 1.0 in order to obtain characteristic values of bond strength, l_b is the bond length of FRP elements and l_e is the optimal bond length of FRP corresponding to the minimal bond length able to carry the maximum anchorage force (f_{mm} indicates masonry average tensile strength).

Finally, the term Γ_{Fk} in (10) represents the characteristic value of the specific fracture energy of the FRP strengthened masonry under a delamination test:

$$\Gamma_{Fd} = c_1 \sqrt{f_{mk} \cdot f_{mm}} \quad [f \text{ in } N/mm^2] \quad (12)$$

where c_1 is an experimentally determined coefficient, that typically may range between 0.015÷0.030 and f_{mk} is the characteristic value of masonry compressive strength.

3.4 The Linear Programming (LP) problem

A linear programming problem is obtained, after some elementary assemblage operations, where the objective function is the total internal power dissipated minus the power dissipated by external loads not dependent on the load multiplier, i.e.:

$$\begin{cases} \min \{ \mathbf{P}_I^{in,ass} \dot{\boldsymbol{\lambda}}^{I,assT} - \mathbf{P}_0^T \mathbf{w} \} \\ \text{such that } \begin{cases} \mathbf{A}^{eq} \mathbf{U} = \mathbf{b}^{eq} \\ \dot{\boldsymbol{\lambda}}^{I,ass} \geq \mathbf{0} \end{cases} \end{cases} \quad (13)$$

where:

- \mathbf{U} is the vector of global unknowns and collects the vector of elements centroids velocities (\mathbf{w}) and rotations (Φ) of both FRP and masonry elements and the vector of assembled interface plastic multiplier rates ($\dot{\boldsymbol{\lambda}}^{I,ass}$). $\dot{\boldsymbol{\lambda}}^{I,ass}$ collects plastic multiplier rates of masonry-masonry interfaces, FRP-FRP interfaces and masonry-FRP interfaces.

- \mathbf{A}^{eq} is the overall constraints matrix and collects normalization conditions, velocity boundary conditions and constraints for plastic flow in velocity discontinuities (on FRP, masonry and FRP-masonry interfaces).

- $\mathbf{P}_I^{in,ass}$ is a row vector that collects contributions to the internal dissipation of masonry-masonry, FRP-FRP and masonry-FRP interfaces.

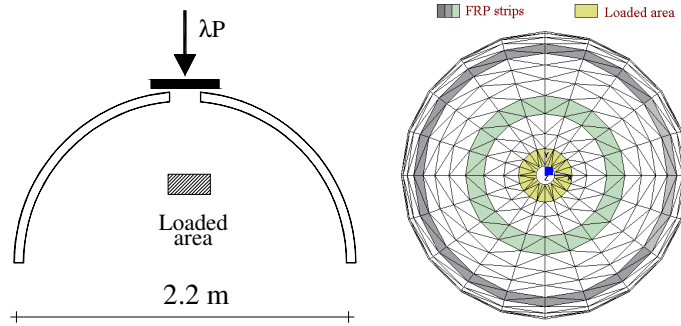


Figure 4: Hemispherical dome. Geometry, loading condition and FE discretization adopted for the numerical analyses.

4 NUMERICAL EXAMPLES:

The example here analyzed relies on a hemispherical dome with inner diameter equal to 2.2 m and thickness of 12 cm and experimentally tested by Foraboschi [9], see Figure 4.

Common Italian bricks of dimensions 120x250x55 mm³ were used, with joints thickness approximately equal to 10 mm. Mechanical properties assumed for joints and bricks are typical of existing masonry in the Northern Italy and the reader is referred to [8][9] there for further details.

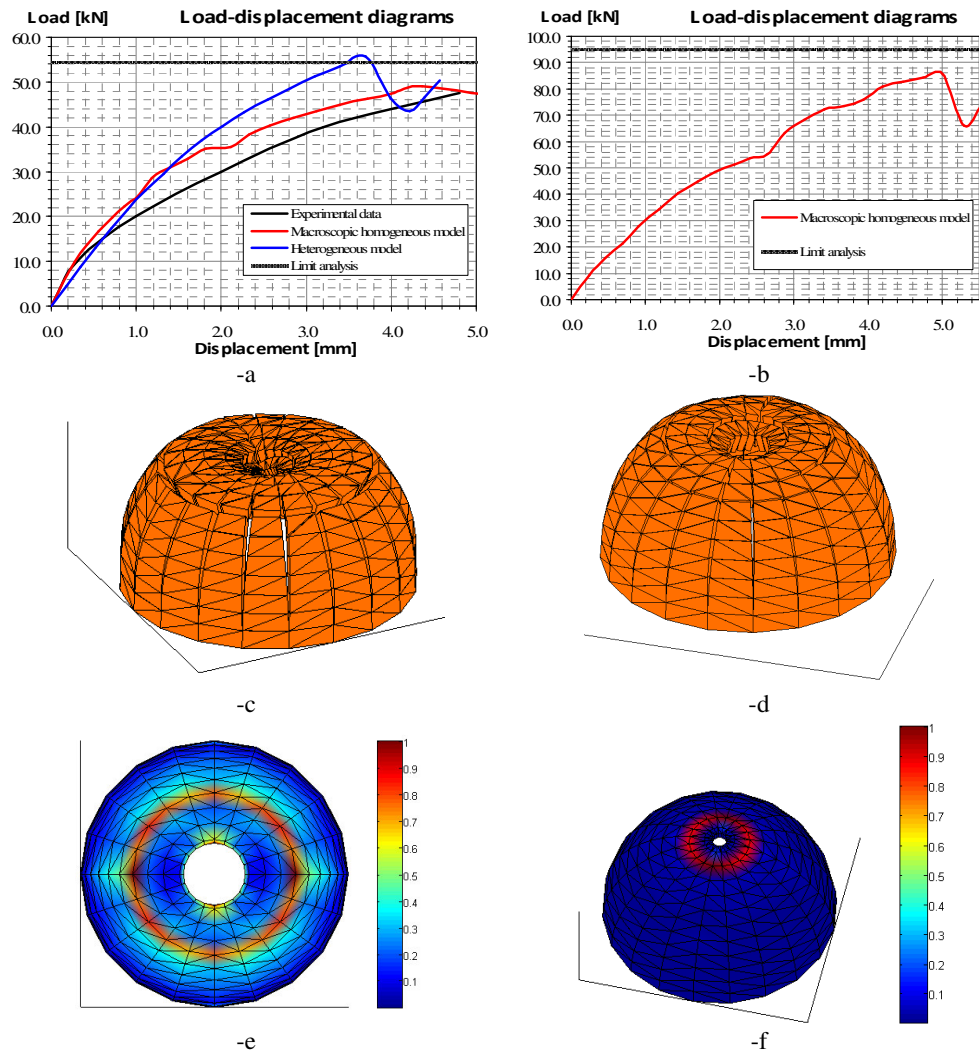


Figure 5: Hemispherical dome. -a and -b: Comparison among collapse loads provided by experimentation, limit analysis and non-linear FE code in absence (-a) and presence (-b) of reinforcement. -c and -d: deformed shapes at collapse from limit analysis (-c: unreinforced case; -d: with FRP). -e and -f: normalized plastic dissipation patch obtained from limit analysis (-e: unreinforced case; -f: with FRP).

In Figure 4, the geometry and the loading condition are represented. The dome is loaded until failure by means of a concentrated vertical increasing load applied at the top of the structure. A steel plate with suitable dimensions is placed between the load and the external loaded surface in order to diffuse vertical stresses. In Figure 5-a and b, load-maximum displacement curves provided by the non-linear model implemented in the commercial code DIANA, experimental data

and limit analysis collapse load are depicted in absence (-a) and presence (-b) of reinforcement. In Figure 5-b and -c, a comparison between deformed shapes near collapse obtained for the unreinforced and FRP reinforced structures is represented. The role played by the strips in changing the failure mechanism is rather evident. Internal plastic dissipation patch is finally represented in Figure 5-c and -d. As can be noted, internal dissipation is concentrated along a circular crown, with the formation of one annular bending hinge. Moreover, an adding amount appears along the meridians of the dome, essentially due to non-zero membrane annular actions. In fact, evident openings along meridians can be observed in the deformed shape. The circumferential FRP strips (see Figure 5-d) play the important role of preventing the formation of meridian cracks, which are partially precluded, with a consequent significant increase of the failure load in presence of fibers. Finally, it is interesting to notice from the deformed shape at collapse that, in presence of reinforcement, failure is more constrained to localize under the zone of application of the external load, with an evident out-of-plane sliding of the loaded area.

References

- [1] Corradi, M., Borri, A., Vignoli, A., “Strengthening techniques tested on masonry structures struck by the Umbria–Marche earthquake of 1997–1998”, *Construction and Building Materials*, **16**, 229–239 (2002).
- [2] Heyman, J., “The safety of masonry arches”, *International Journal of Mechanical Sciences*, **43**, 209-224 (1969).
- [3] Sinha, B.P., “A simplified ultimate load analysis of laterally loaded model orthotropic brickwork panels of low tensile strength”, *Jour. Struct. Eng. ASCE*, 56B(4), 81-84 (1978).
- [4] Orduña, A., Lourenço, P.B., “Three-dimensional limit analysis of rigid blocks assemblages. Part I: Torsion failure on frictional joints and limit analysis formulation”, *Int. J. Sol. and Struct.*, **42 (18-19)**, 5140-5160 (2005).
- [5] Milani, E., Milani, G., Tralli, A., “Limit analysis of masonry vaults by means of curved shell finite elements and homogenization”, *Int. J. Sol. and Struct.*, **45**, 5258-5288 (2008).
- [6] Caporale, A., Luciano, R., Rosati, L., “Limit analysis of masonry arches with externally bonded FRP reinforcements”, *Comp. Meth. Appl. Mech. Eng.*, **196**, 247-260 (2006).
- [7] CNR-DT200 2006, “Guide for the design and construction of externally bonded FRP systems for strengthening existing structures”, *C.N.R., National Research Council*, Italy, 2006.
- [8] Milani, G., Milani, E., Tralli, A., “Upper Bound homogenized limit analysis of FRP-reinforced masonry curved structures. Part I: unreinforced masonry failure surfaces; Part II: structural analyses”, *in press in Computers & Structures* (2009).
- [9] Foraboschi, P., “Masonry structures externally reinforced with FRP strips: tests at the collapse [in Italian]”, In: *Proc. I Convegno Nazionale “Sperimentazioni su Materiali e Strutture”*, Venice, 2006.
- [10] Suquet, P., "Analyse limite et homogeneisation" *Comptes Rendus de l'Academie des Sciences - Series IIB – Mechanics*, **296**, 1355-1358 (1983).
- [11] Krabbenhoft, K., Lyamin, A.V., Hjiij, M., Sloan, S.W., “A new discontinuous upper bound limit analysis formulation”, *International Journal for Numerical Methods in Engineering*, **63**, 1069-1088 (2005).